

The American Journal of Human Genetics, Volume 107

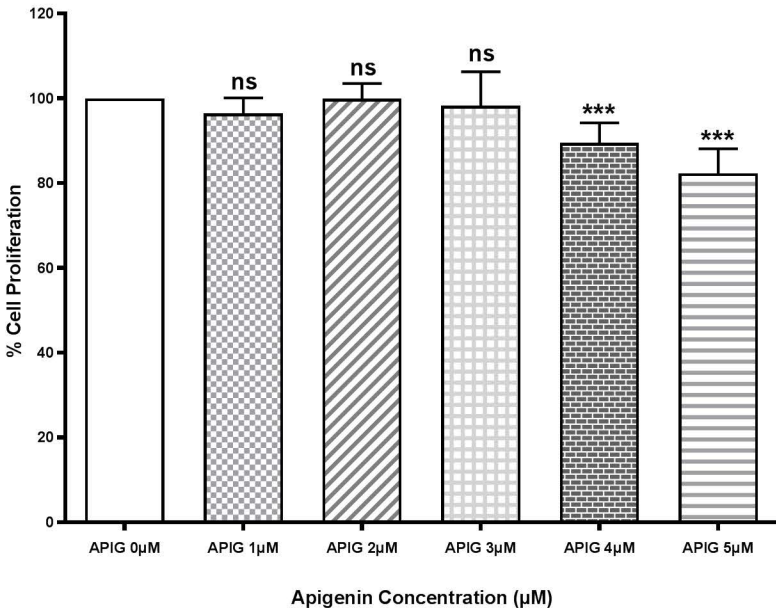
Supplemental Data

**Apigenin as a Candidate Prenatal Treatment for
Trisomy 21: Effects in Human Amniocytes and
the Ts1Cje Mouse Model**

Faycal Guedj, Ashley E. Siegel, Jeroen L.A. Pennings, Fatimah Alsebaa, Lauren J. Massingham, Umadevi Tantravahi, and Diana W. Bianchi

All Amniocytes Combined

A



B

Euploid Versus Trisomie 21 Amniocytes

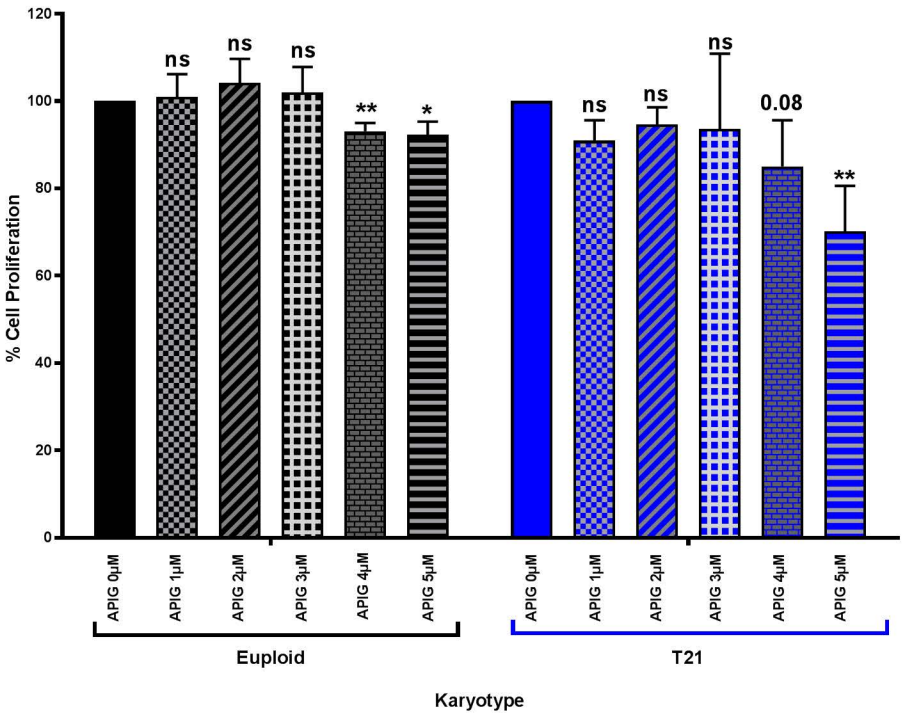


Figure S 1: Effects of apigenin on cell proliferation in T21 and euploid amniocytes. Cell proliferation was measured using two different assays and normalized to 100 % in untreated cells. Effect of apigenin were analyzed on all the cell lines together **(A)** or separated by genotype **(B)**. High doses of apigenin induced significantly reduced cell proliferation in euploid (4-5 μM) and T21 (5 μM) amniocytes. * ($p < 0.05$), ** ($p < 0.01$), *** ($p < 0.001$).

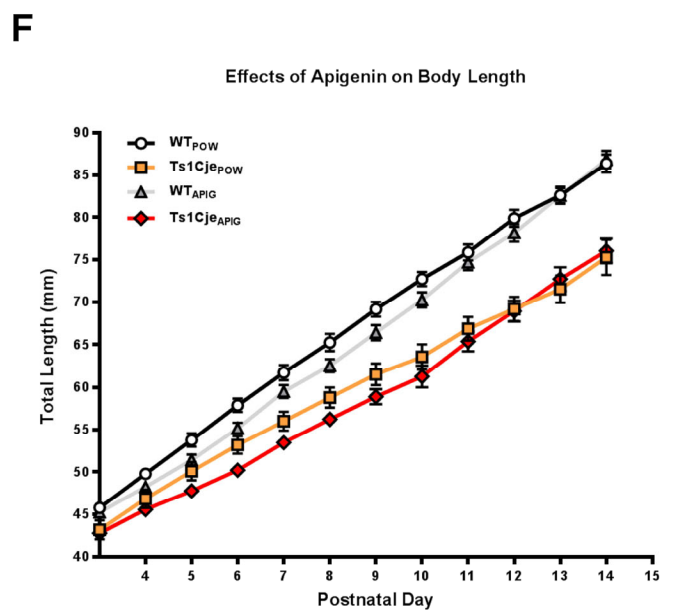
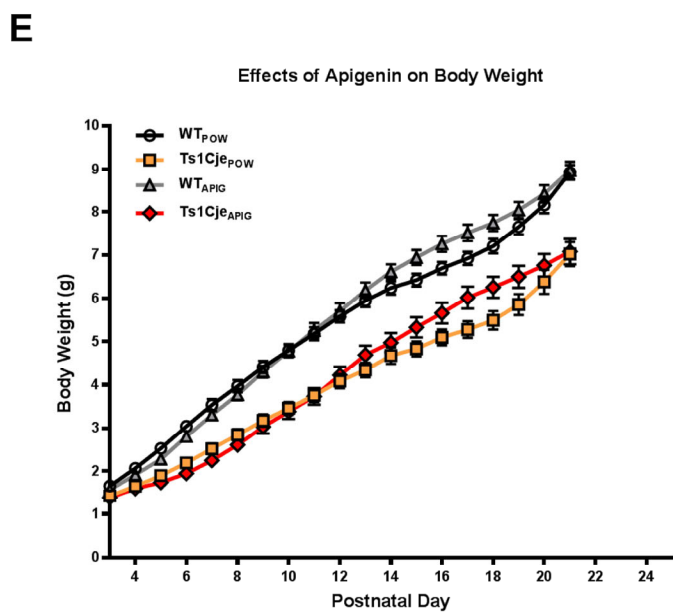
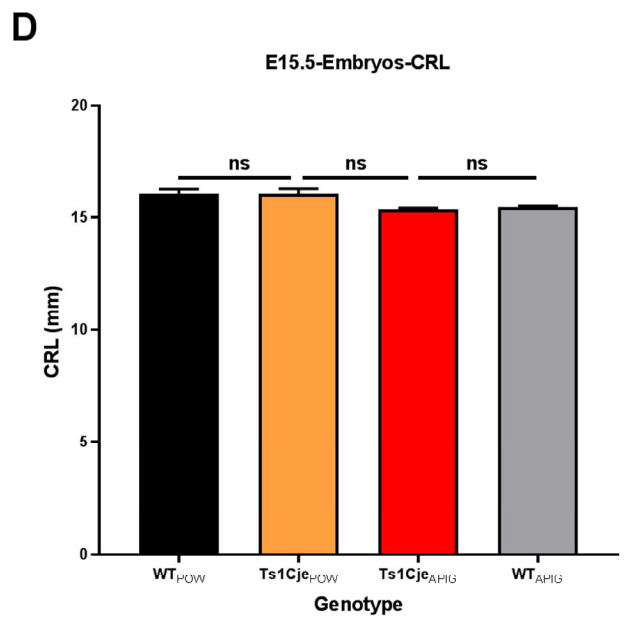
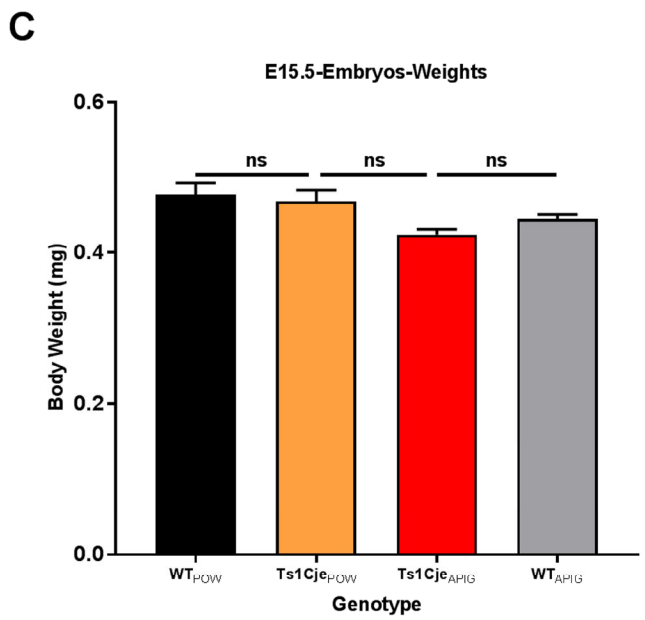
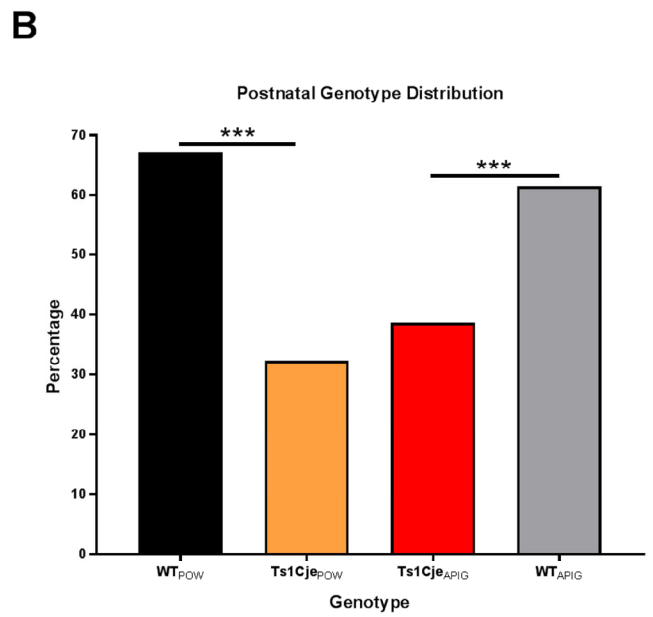
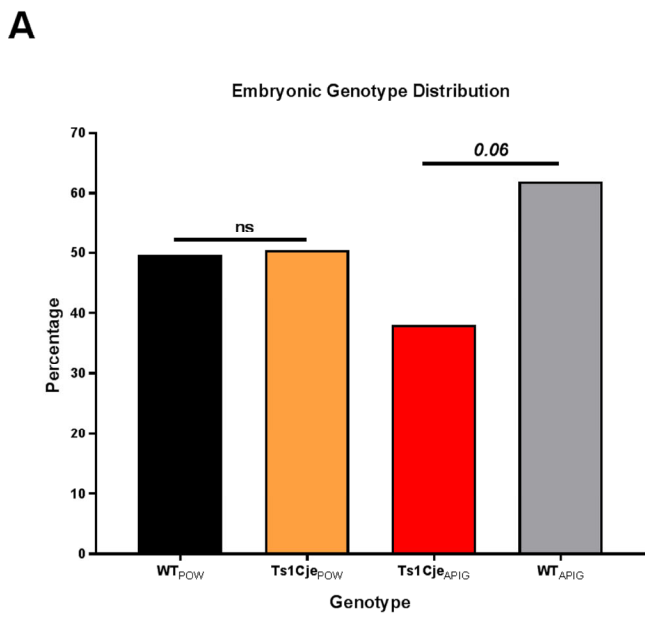


Figure S 2: Effects of apigenin on natural history and growth in Ts1Cje and WT littermates.

(A-B) Embryonic and postnatal genotype distribution in untreated and apigenin-treated mice.

Genotype distribution in the untreated group followed mendelian inheritance while only 32.8% of the neonates were Ts1Cje postnatally. In the apigenin-treated group, 38% of embryos were Ts1Cje and 62% were WT. Postnatally, the genotype distribution was similar in the untreated and apigenin-treated.

(C-F) Embryonic and postnatal growth in untreated and apigenin-treated mice.

Apigenin treatment did not result in significant changes in the growth profiles in Ts1Cje and WT mice.

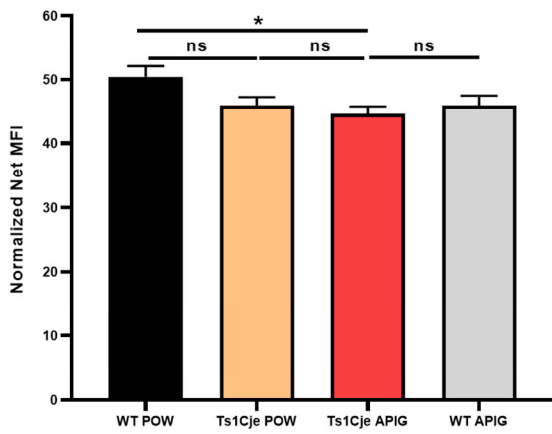
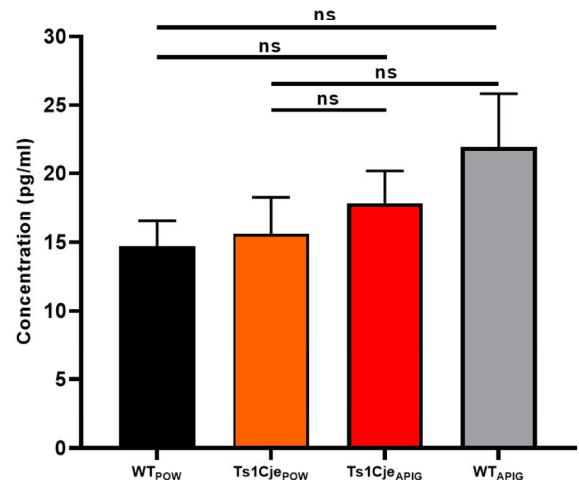
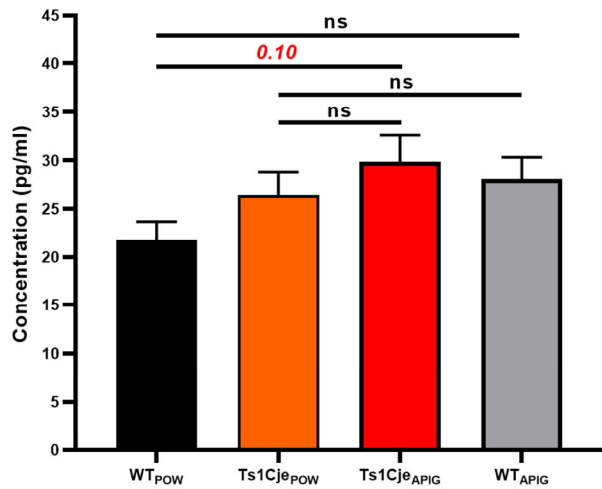
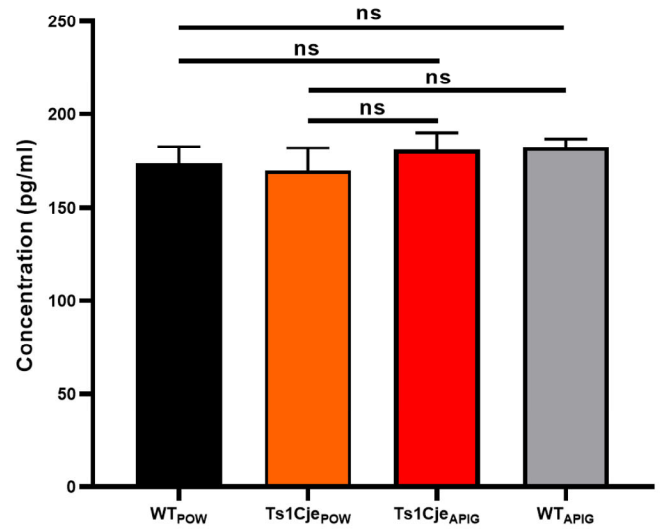
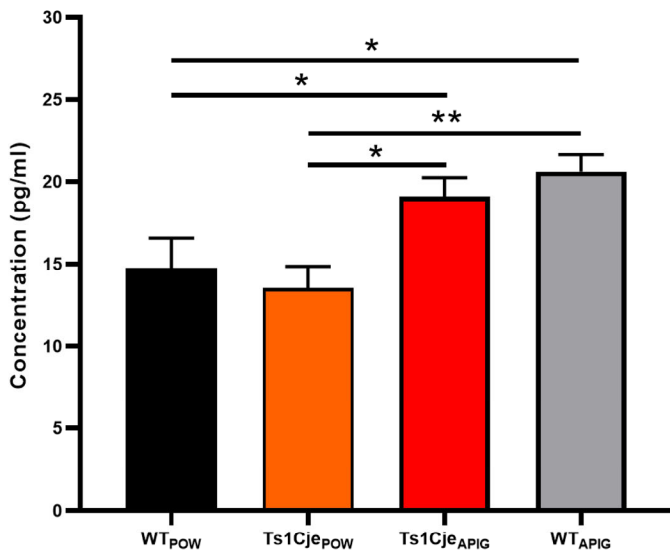
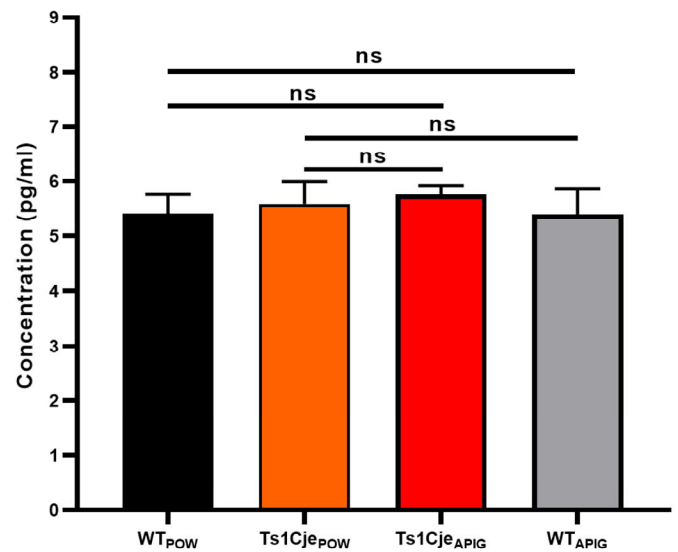
A**NFKB Total Proteins-Apigenin-Cortex****B****Ts1Cje-Apigenin-IFNG-Cortex****C****Ts1Cje-Apigenin-IL12P40-Cortex****D****Ts1Cje-Apigenin-IL1A-Cortex****E****Ts1Cje-Apigenin-IL10-Cortex****F****Ts1Cje-Apigenin-VEGF-Cortex**

Figure S 3: Effects of apigenin treatment on inflammatory, angiogenesis and neurotrophic proteins in Ts1Cje and WT adult cerebral cortex. Luminex technology was used to analyze the expression of inflammatory proteins NFκB (A), IFNG (B), IL12P40 (C), IL1A (D), IL10 (E), and pro-angiogenic VEGF (F) in the adult cerebral cortex of (WT_{Pow}=10, Ts1Cje_{Pow}=11, WT_{Apig}=9, Ts1Cje_{Apig}=9).

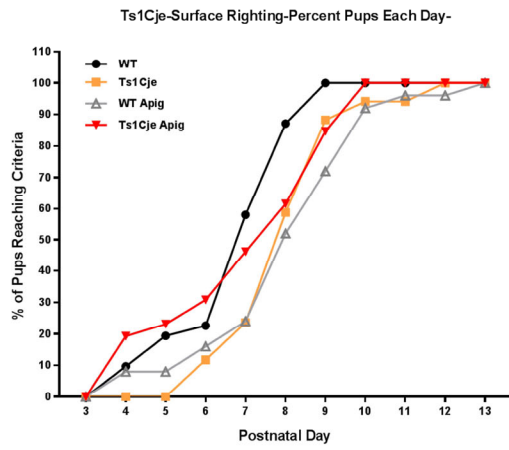
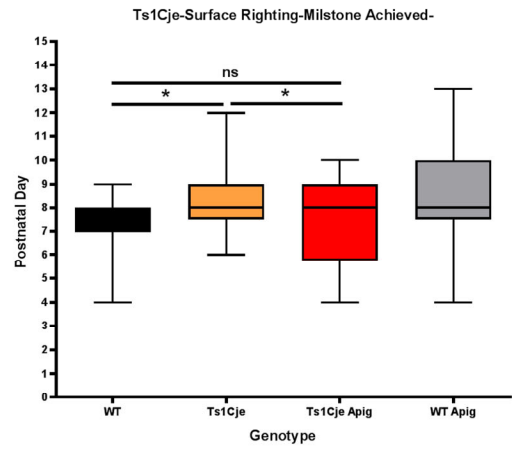
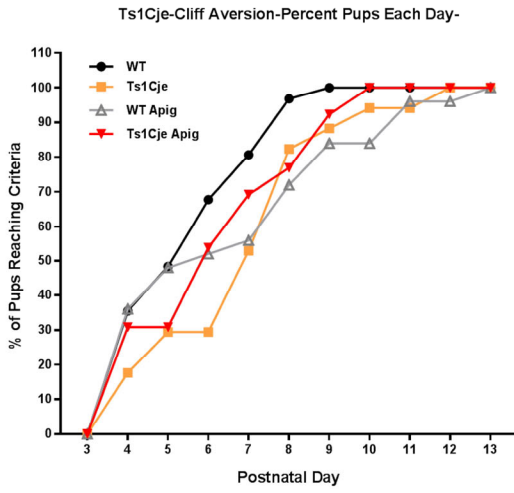
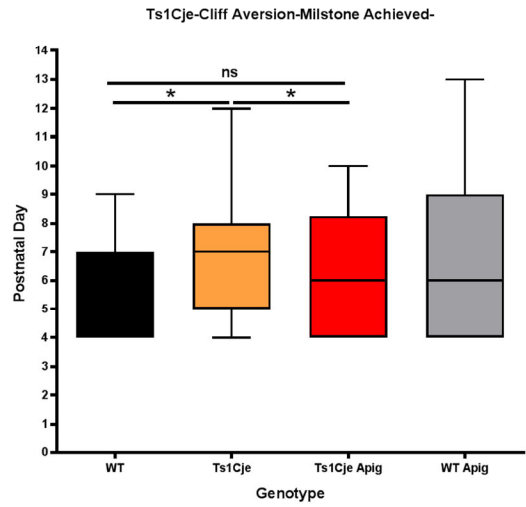
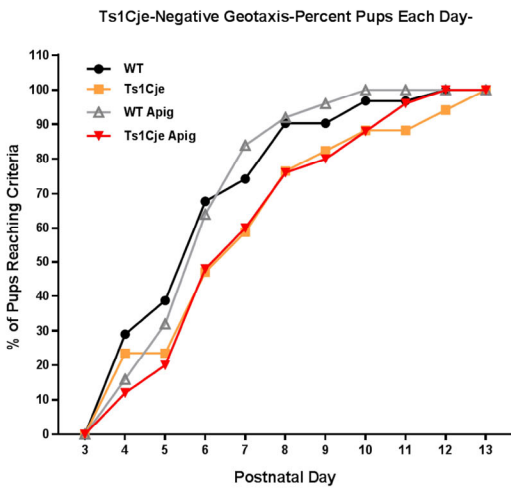
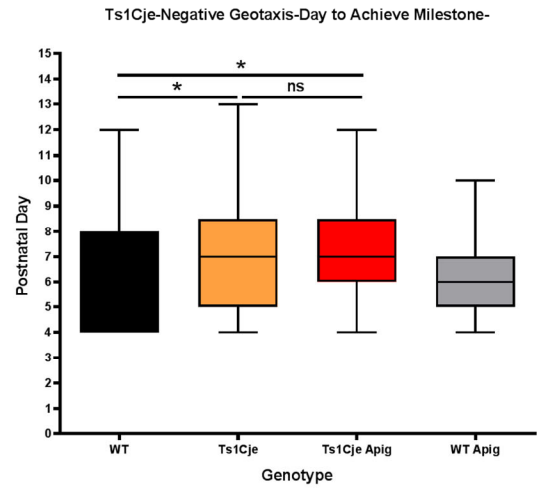
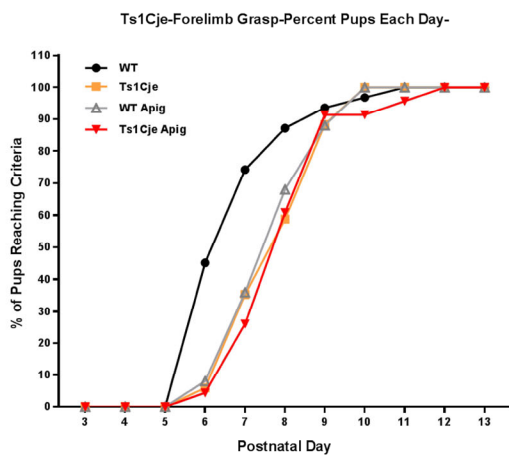
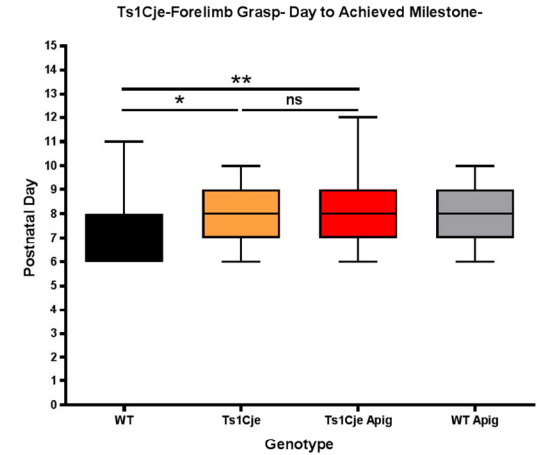
A**B****C****D****E****F****G****H**

Figure S 4: Effects of apigenin on early developmental milestones in Ts1Cje and WT littermates. Untreated Ts1Cje neonates exhibit significant delays in early milestones, including surface righting (**A-B**), cliff aversion (**C-D**), negative geotaxis (**E-F**) and forelimb grasp (**G-H**). Apigenin treatment partially improved Ts1Cje performance in surface righting and cliff aversion but did not affect performance in negative geotaxis and forelimb grasp tests.

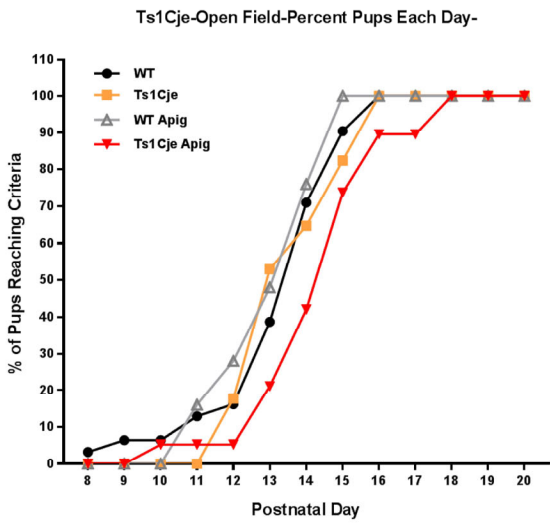
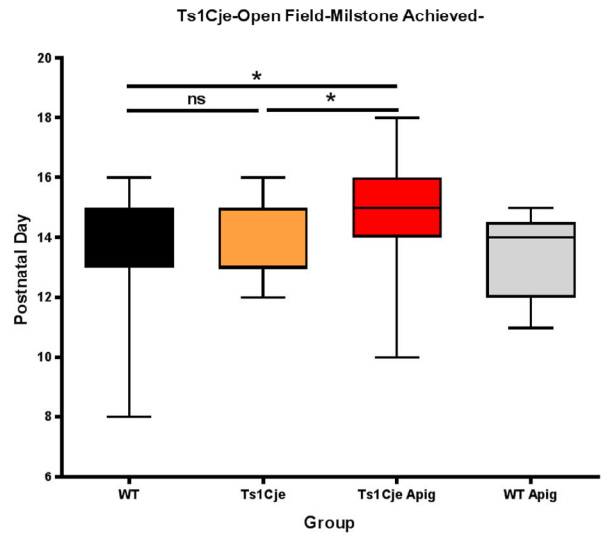
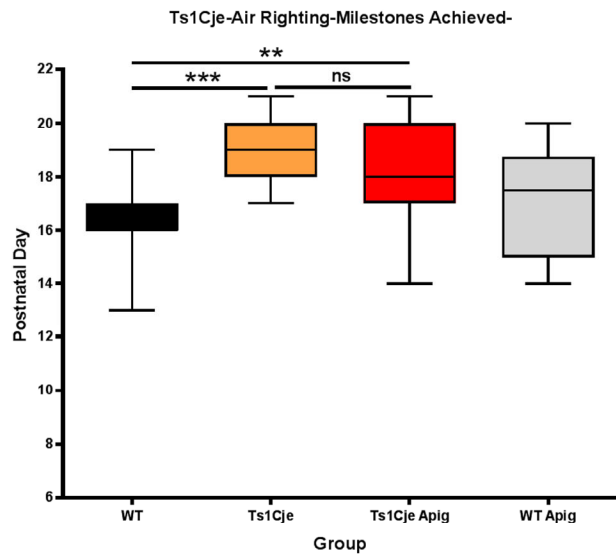
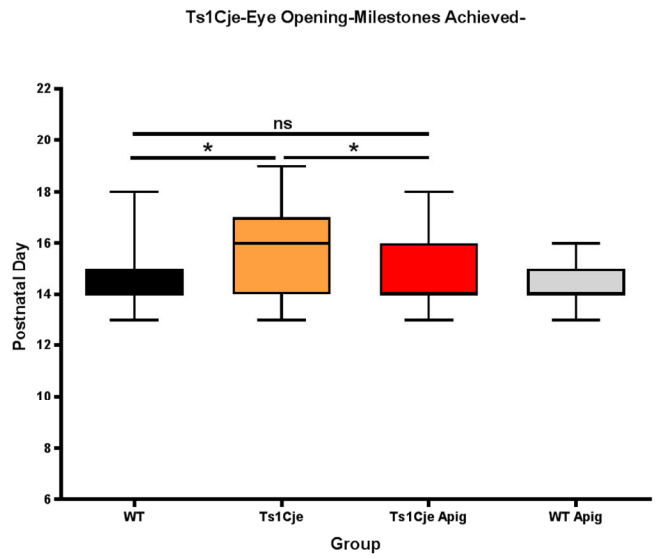
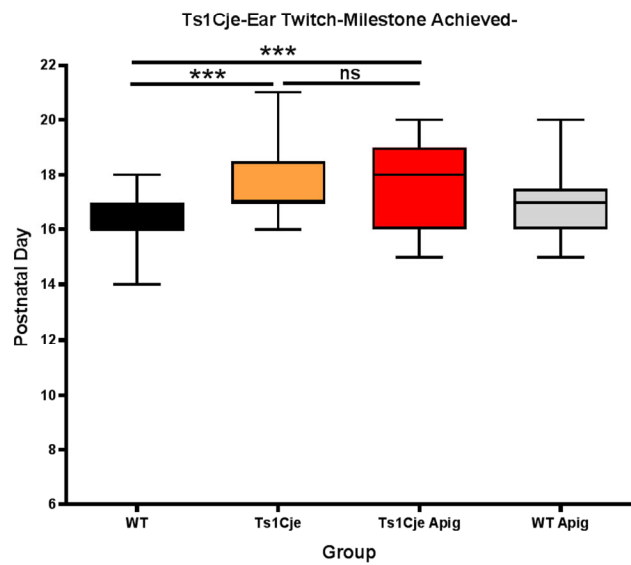
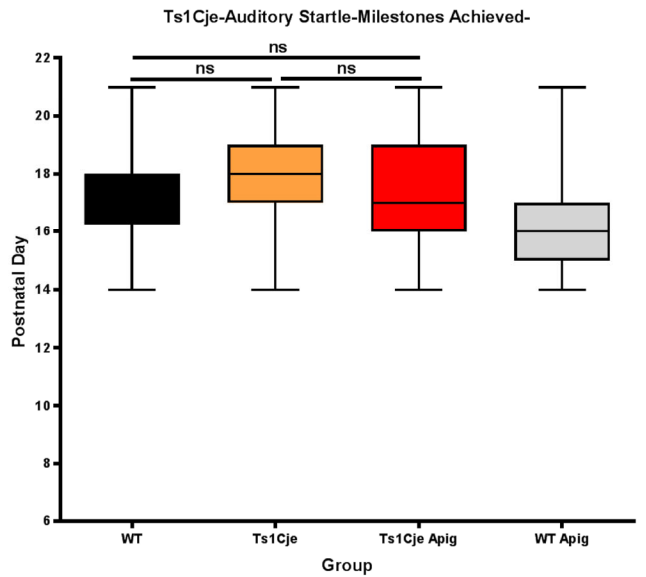
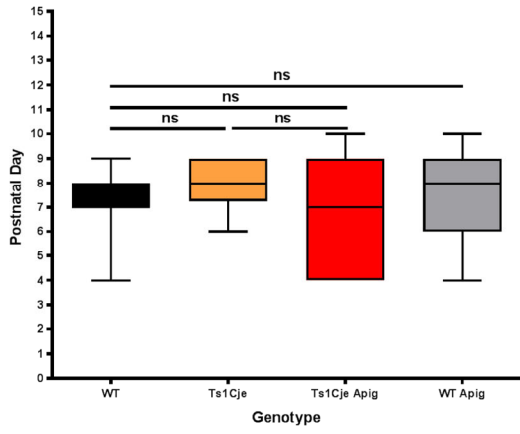
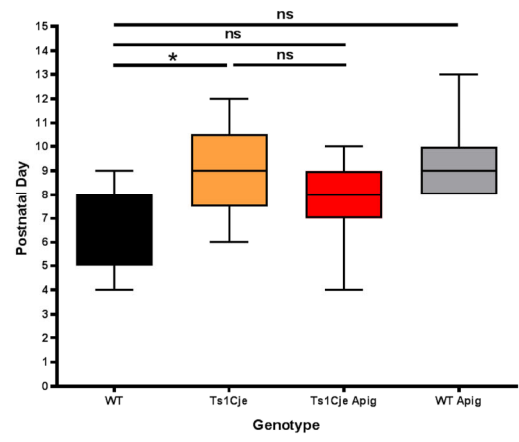
A**B****C****D****E****F**

Figure S 5: Effects of apigenin on late developmental milestones in Ts1Cje and WT littermates. Ts1Cje neonates exhibit significant delays in late milestones, including air righting (**C**), eye opening (**D**), ear twitch (**E**). Apigenin treatment partially improved air righting and eye opening, but negatively affected motor development (open field).

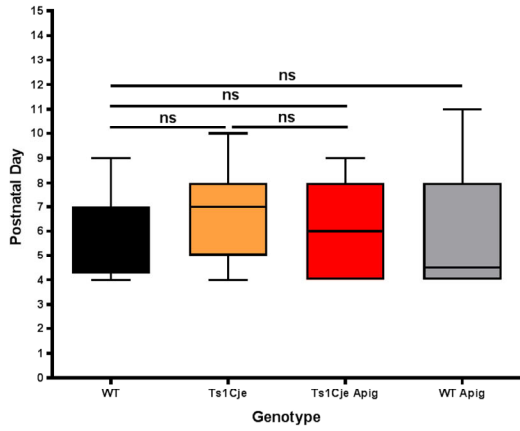
Ts1Cje-Surface Righting-Males-



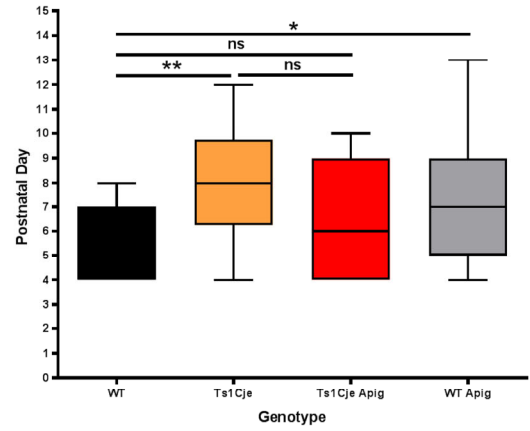
Ts1Cje-Surface Righting-Females-



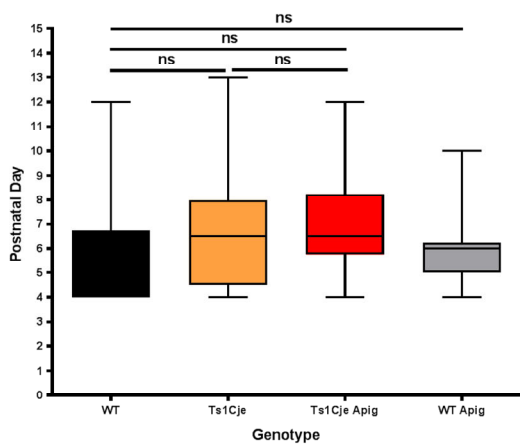
Ts1Cje-Cliff Aversion-Males-



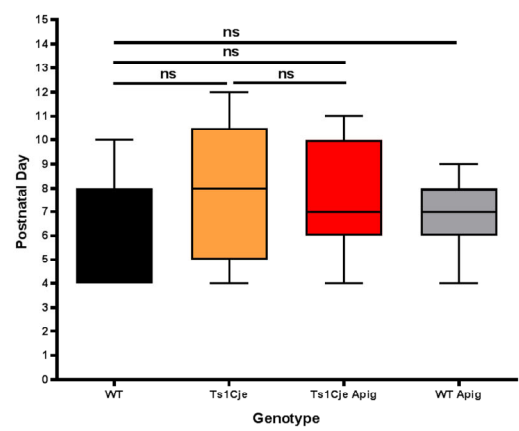
Ts1Cje-Cliff Aversion-Females-



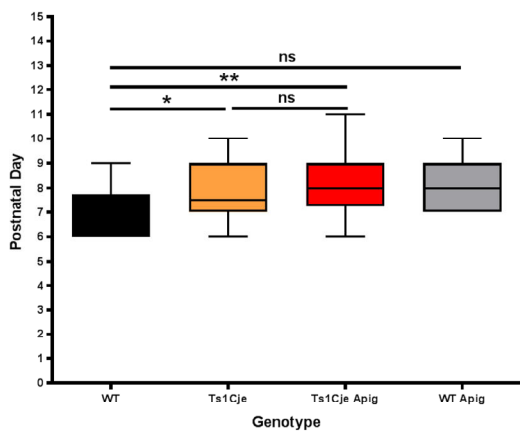
Ts1Cje-Negative Geotaxis-Males-



Ts1Cje-Negative Geotaxis-Females-



Ts1Cje-Forelimb Grasp-Males-



Ts1Cje-Forelimb Grasp-Females-

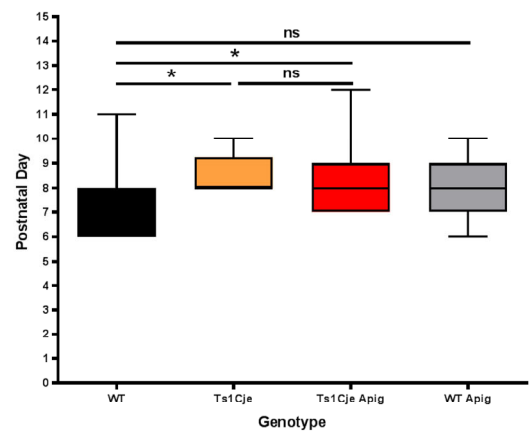


Figure S 6: Sex-Specific Effects of apigenin on early developmental milestones in Ts1Cje and WT littermates.

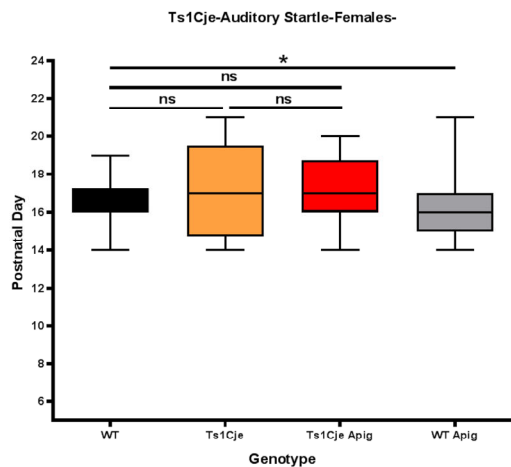
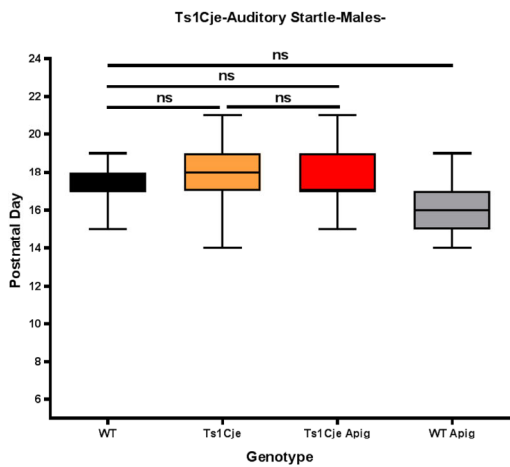
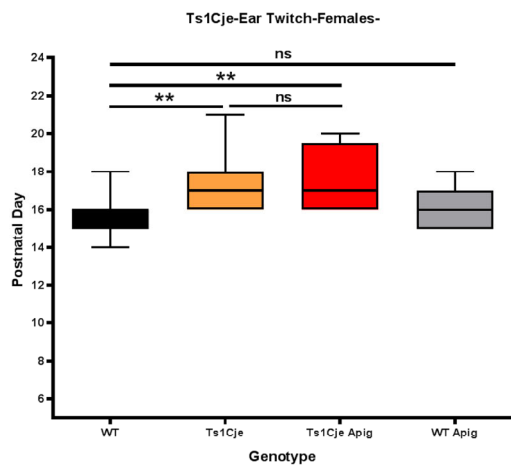
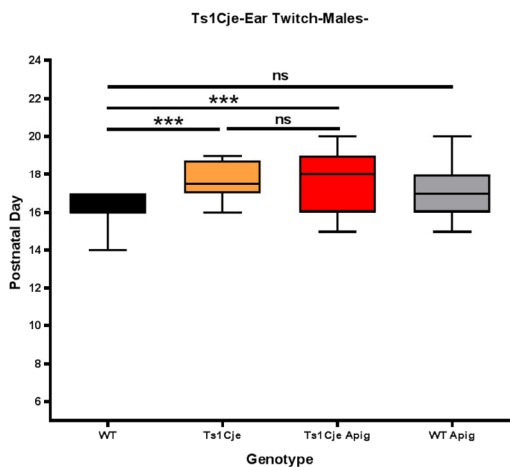
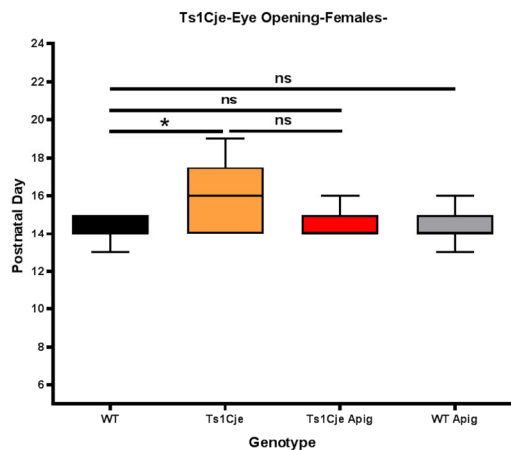
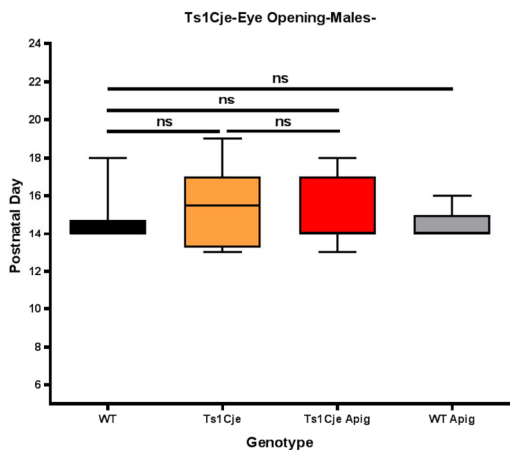
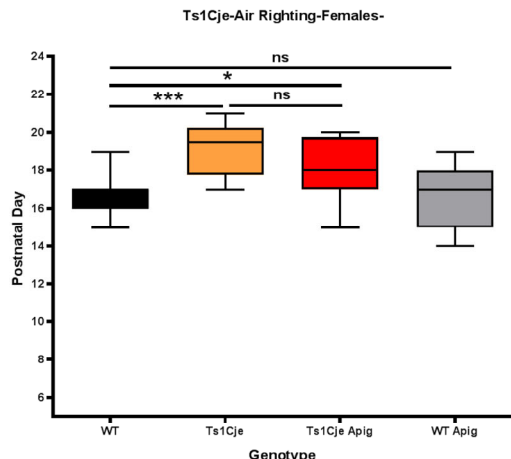
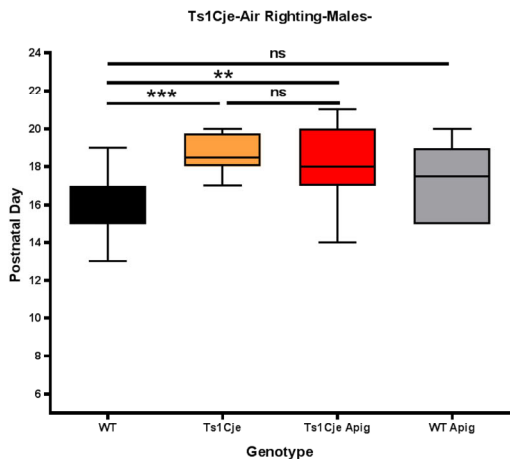


Figure S 7: Sex-Specific Effects of apigenin on late developmental milestones in Ts1Cje and WT littermates.

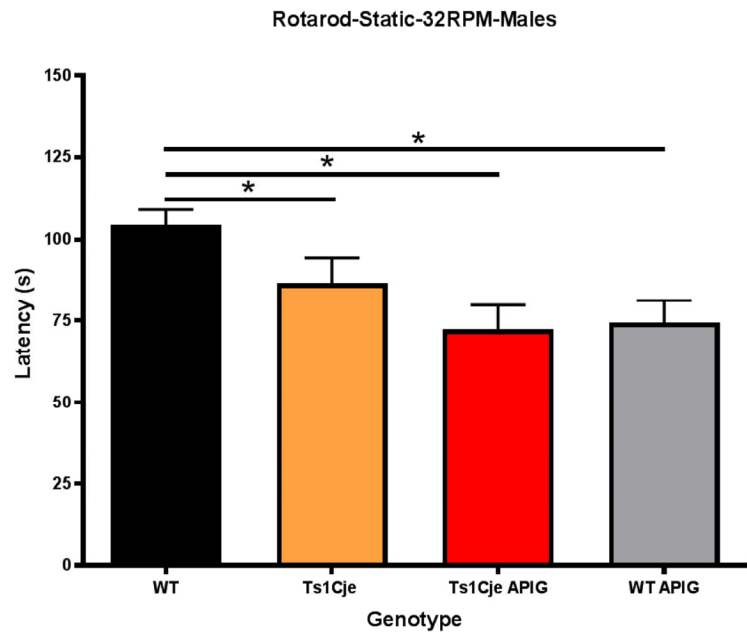
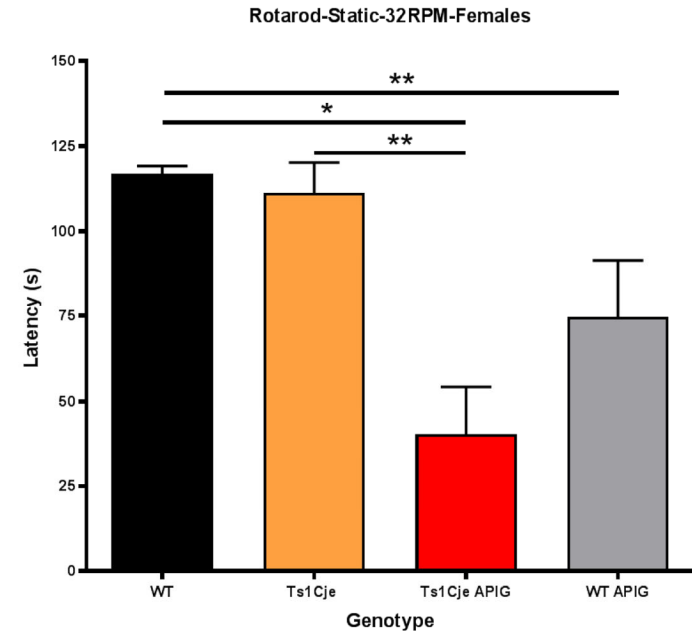
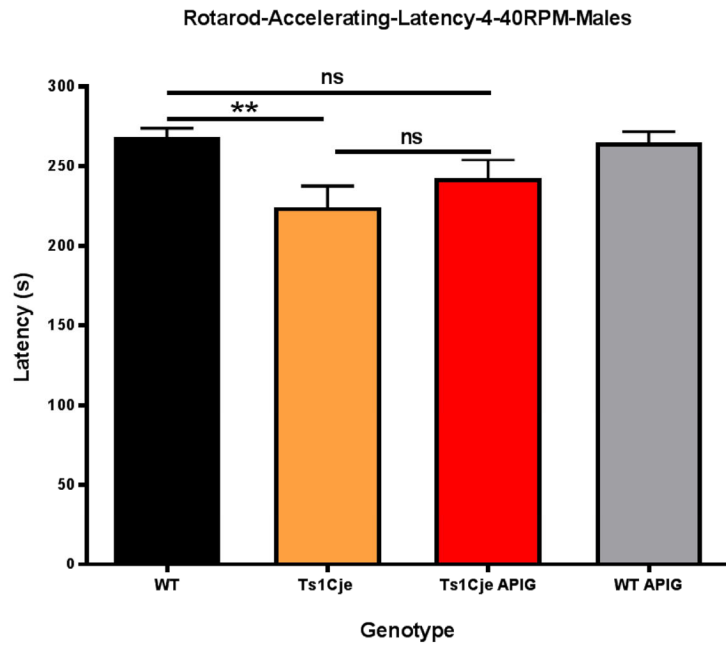
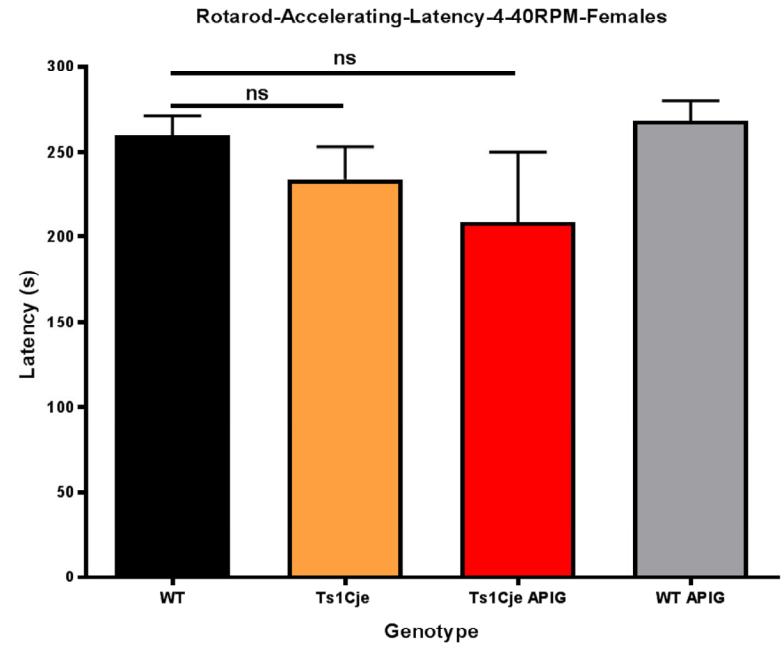
A**B****C****D**

Figure S 8: Adverse effects of apigenin on motor coordination in untreated and apigenin-treated adult Ts1Cje and WT males and females. Motor coordination was analyzed using the rotarod test in untreated and apigenin-treated WT and Ts1Cje males (WT_{Pow}=13, Ts1Cje_{Pow}=12, WT_{Apig}=17, Ts1Cje_{Apig}=16) and females (WT_{Pow}=8, Ts1Cje_{Pow}=7, WT_{Apig}=14, Ts1Cje_{Apig}=12). **(A-B)** Performance of untreated and apigenin-treated Ts1Cje and WT male and female mice in the static speed trial at 32 RPM. **(C-D)** Performance of untreated and apigenin-treated Ts1Cje and WT male and female mice in the accelerating speed trial (4-40 RPM). Ts1Cje males exhibited significant motor coordination deficits (fell off the rotarod faster) compared to their WT littermates, however, motor coordination was not significantly affected in Ts1Cje female mice. Apigenin treatment had negative effects on motor coordination in both WT and Ts1Cje male and female mice. * (p<0.05), ** (p<0.01), *** (p<0.001).

SUPPLEMENTARY TABLES

Table S 1: Karyotype and gestational age information of the human trisomy 21 (T21) and euploid amniocytes pairs used in this study. This table is included in the Supplementary Materials Word document.

Table S 2: Effects of apigenin on differentially expressed (DEX) genes in age and sex-matched T21 and euploid amniocytes. (2A) List of DEX genes in T21 versus euploid amniocytes. **(2B)** Regulatory effects of apigenin treatment on chromosome 21 genes in T21 amniocytes. **(2C)** List of DEX genes induced by apigenin treatment in T21 amniocytes.

Table S 3: Marginally expressed (MEX) genes (Top 1% up-and down-regulated genes) in untreated and apigenin-treated T21 and euploid amniocytes. (3A) List of MEX genes specifically up- and down-regulated after apigenin treatment. **(3B)** List of MEX genes in untreated human T21 versus euploid amniocytes. **(3C)** List of MEX genes in apigenin-treated T21 compared to untreated T21 amniocytes. **(3D)** List of MEX genes in apigenin-treated T21 amniocytes compared to untreated euploid amniocytes. **(3E)** List of MEX genes in apigenin-treated euploid compared to untreated euploid amniocytes. Up-regulated genes are highlighted in “Red” and down-regulated genes in “Blue” and the percent of gene expression change is indicated for each comparison.

Table S 4: Summary of DAVID dysregulated pathways in untreated and apigenin-treated T21 and euploid amniocytes. (4A) DAVID dysregulated pathways in untreated human T21 versus euploid amniocytes. **(4B)** DAVID dysregulated pathways in apigenin-treated T21 compared to untreated T21 amniocytes. **(4C)** DAVID dysregulated pathways in apigenin-treated

T21 amniocytes compared to untreated euploid amniocytes. **(4D)** DAVID dysregulated pathways in apigenin-treated euploid compared to untreated euploid amniocytes.

Table S 5: Summary of GSEA dysregulated pathways in untreated and apigenin-treated T21 and euploid amniocytes. (5A) GSEA dysregulated pathways in untreated human T21 versus euploid amniocytes. **(5B)** GSEA dysregulated pathways in apigenin-treated T21 compared to untreated T21 amniocytes. **(5C)** GSEA dysregulated pathways in apigenin-treated T21 amniocytes compared to untreated euploid amniocytes. **(5D)** GSEA dysregulated pathways in apigenin-treated euploid compared to untreated euploid amniocytes.

Table S 6: Summary of IPA dysregulated pathways in untreated and apigenin-treated T21 and euploid amniocytes. (6A) IPA dysregulated pathways in untreated human T21 versus euploid amniocytes. **(6B)** IPA dysregulated pathways in apigenin-treated T21 compared to untreated T21 amniocytes. **(6C)** IPA dysregulated pathways in apigenin-treated T21 amniocytes compared to untreated euploid amniocytes. **(6D)** IPA dysregulated pathways in apigenin-treated euploid compared to untreated euploid amniocytes.

Table S 7: Summary of IPA predicted upstream regulators in untreated and apigenin-treated T21 amniocytes. (7A) IPA predicted upstream regulators in untreated human T21 versus euploid amniocytes. **(7B)** in apigenin-treated T21 compared to untreated T21 amniocytes. **(7C)** IPA predicted upstream regulators in apigenin-treated T21 amniocytes compared to untreated euploid amniocytes. **(7D)** IPA predicted upstream regulators in apigenin-treated euploid compared to untreated euploid amniocytes.

Table S 8: Effects of apigenin on DEX genes in Ts1Cje and WT E15.5 forebrain. (8A) Regulatory effects of apigenin treatment on the DEX genes in untreated Ts1Cje E15.5 forebrain.

(8B) DEX Genes in apigenin-treated Ts1Cje compared to apigenin-treated E15.5 forebrain. **(8C)** DEX genes in apigenin-treated Ts1Cje and WT E15.5 forebrain compared to their untreated counterparts.

Table S 9: MEX genes in untreated and apigenin-treated Ts1Cje and WT E15.5 forebrain.

(9A) MEX genes in untreated Ts1Cje compared to untreated WT embryonic forebrain. **(9B)** MEX genes in apigenin-treated WT compared to untreated WT embryonic forebrain. **(9C)** MEX genes in apigenin-treated Ts1Cje compared to untreated WT embryonic forebrain. **(9D)** MEX genes in apigenin-treated Ts1Cje compared to apigenin-treated WT embryonic forebrain. **(9E)** MEX genes in apigenin-treated Ts1Cje compared to untreated Ts1Cje embryonic forebrain. Up-regulated genes are highlighted in “Red” and down-regulated genes in “Blue” and the percent of expression change is indicated for each comparison.

Table S 10: Summary of DAVID dysregulated pathways in untreated and apigenin-treated

Ts1Cje and WT E15.5 forebrain. (10A) DAVID dysregulated pathways in Ts1Cje compared to untreated WT embryonic forebrain. **(10B)** DAVID dysregulated pathways in apigenin-treated Ts1Cje compared to untreated Ts1Cje embryonic forebrain. **(10C)** DAVID dysregulated pathways in apigenin-treated Ts1Cje compared to untreated WT embryonic forebrain. **(10D)** DAVID dysregulated pathways in apigenin-treated WT compared to untreated WT embryonic forebrain.

Table S 11: Summary of GSEA dysregulated pathways in untreated and apigenin-treated

Ts1Cje and WT E15.5 forebrain. (11A) GSEA dysregulated pathways in Ts1Cje compared to untreated WT embryonic forebrain. **(11B)** GSEA dysregulated pathways in apigenin-treated Ts1Cje compared to untreated Ts1Cje embryonic forebrain. **(11C)** GSEA dysregulated pathways in apigenin-treated Ts1Cje compared to untreated WT embryonic forebrain. **(11D)** GSEA

dysregulated pathways in apigenin-treated WT compared to untreated WT embryonic forebrain.

Table S 12: Summary of IPA dysregulated pathways in untreated and apigenin-treated Ts1Cje and WT E15.5 forebrain. (12A) IPA dysregulated pathways in Ts1Cje compared to untreated WT embryonic forebrain. **(12B)** IPA dysregulated pathways in apigenin-treated Ts1Cje compared to untreated Ts1Cje embryonic forebrain. **(12C)** IPA dysregulated pathways in apigenin-treated Ts1Cje compared to untreated WT embryonic forebrain. **(12D)** IPA dysregulated pathways in apigenin-treated WT compared to untreated WT embryonic forebrain.

Table S 13: Summary of IPA predicted upstream regulators in untreated and apigenin-treated Ts1Cje and WT E15.5 forebrain. (13A) IPA predicted upstream regulators in Ts1Cje compared to untreated WT embryonic forebrain. **(13B)** IPA predicted upstream regulators in apigenin-treated Ts1Cje compared to untreated Ts1Cje embryonic forebrain. **(13C)** IPA predicted upstream regulators in apigenin-treated Ts1Cje compared to untreated WT embryonic forebrain. **(13D)** IPA predicted upstream regulators in apigenin-treated WT compared to untreated WT embryonic forebrain.

I- Supplementary Methods:

1. In Vitro Studies:

Human Amniocytes

The amniocytes were obtained after clinically indicated prenatal karyotyping. As this was discarded material that was de-identified, patient consent was deemed unnecessary. Only fetal karyotype and sex were known. Second trimester amniocytes were prepared as described previously (21). All trisomy 21 samples used in this study have full T21 and no mosaic or partial trisomy samples were used. Samples were matched for sex and gestational age according to the following table:

Table S 1: Karyotype and Gestational Age Information of the Human Trisomy 21 and Euploid Amniocytes Pairs Used in this Study.

Pair	Sample ID	Gestational Age	Karyotype	Sex
Pair 1	JJ1298	16 + 1/7	46XX, 2N	Female Pair
	CG16-467	16 + 5/7	47XX, T21	
Pair 2	JT1275	16 + 2/7	46XX, 2N	Female Pair
	JG16-213	16 + 1/7	47XX, T21	
Pair 3	KM1170	19 + 5/7	46XX, 2N	Female Pair
	BB16-225	19 + 6/7	47XX, T21	
Pair 4	CV1166	15 + 4/7	46XY, 2N	Male Pair
	SZ16-201	15 + 3/7	47XY, T21	
Pair 5	ER48	19 + 6/7	46XY, 2N	Male Pair
	JL779	19 + 4/7	47XY, T21	

Pair 6	ML181	18 + 3/7	46XY, 2N	Male Pair
	BB1174	18 + 3/7	47XY, T21	
Pair 7	LC847	17 + 3/7	46XY, 2N	Male Pair
	SG01	18 + 4/7	47XY, T21	

Apigenin Optimal Dose Selection Using Cell Proliferation Assays

Amniocytes (10^{+5} cells) from fetuses with DS and euploid controls were plated in duplicate in 24-well plate culture dishes and incubated overnight at 37°C (20% O₂, 5% CO₂). The following day, cells were either left untreated or treated with five different concentrations of apigenin (1, 2, 3, 4 and 5 µM). Cell culture media (AmnioMax C-100 Complete, Thermo Fisher Scientific, Waltham, MA) and apigenin-containing AmnioMax C-100 Complete media were freshly prepared and changed daily during the treatment periods.

Cell proliferation was evaluated using the CellTiter 96[®] Aqueous cell proliferation assay according to the manufacturer's instructions (Promega, Madison, WI). Absorbance at 490 nm was measured using the Synergy 2 well plate reader (BioTek®, Winooski, VT). Results were normalized to 100 % for untreated cells for further comparison with apigenin-treated cells. Automatic cell counts were performed using the Scepter™ 2.0 Handheld Automated Cell Counter and the 60 µM sensors (EMD Millipore, Billerica, MA).

Oxidative Stress and Antioxidant Capacity

Amniocytes were incubated with media alone or apigenin for three consecutive days, with media and drug prepared freshly and changed daily. At the end of the treatment, efficacy was evaluated using cell proliferation, antioxidant capacity, oxidative stress and global gene expression as the endpoints.

The Comet assay or Single Cell Gel Electrophoresis (SCGE) uses a DNA-binding fluorescent dye.

Because of oxidative stress, damaged DNA extrudes from the nucleus making a “tail”. The assay calculates the relative amount of DNA in the “tail” versus the nucleus “head”. The Comet assay was performed using the CometAssay® kit according to the manufacturer’s instructions (Trevigen, Gaithersburg, MD).

To measure the physiological responses to oxidative stress before and after apigenin treatment, cells were centrifuged (1,100 g for 5 min), rinsed with ice cold 1X PBS and centrifuged again at 1,100 g for 5 min. The cell pellet was used for protein extraction using the NucleoSpin RNA/Protein extraction kit (Macherey-Nagel, Bethlehem, PA), and protein concentration was determined using the Pierce™ BCA protein assay kit (Thermo Fisher Scientific, Cambridge, MA). 5,000 µg of total protein was used to measure the total antioxidant capacity using the OxiSelect™ Total Antioxidant Capacity (TAC) assay kit according to the manufacturer’s instructions (CellBiolabs, San Diego, CA).

RNA Extraction and Microarray Hybridization

For gene expression studies, amniocytes were incubated with media alone or 2 µM apigenin for three consecutive days. Cells were then rinsed with ice cold PBS 1X (-Ca²⁺, -Mg²⁺) and centrifuges at 1000 RPM for 5 min. The cell pellet was used for RNA extraction using NucleoSpin RNA/Protein extraction (Macherey-Nagel, Bethlehem, PA). RNA was processed and hybridized on the GeneChip® Human Transcriptome HT 2.0 array according to the manufacturer’s instructions (Affymetrix, Santa Clara, CA). Each array corresponded to labeled cDNA from one amniocyte culture.

Array data were normalized using the oligo R package. Of the 70492 probe sets on the array, only the 42935 gene-coding probe sets were used in further analyses. Results were further visualized using a Principal Component Analysis (PCA) as well as heatmap combined with hierarchical clustering. For pathway analyses, the 42935 probe sets were first collapsed to 33721 unique genes to remove gene-level redundancy.

After that pathway analyses were carried out using the Database of Annotation, Visualization, and Integrated Discovery (DAVID), Ingenuity Pathway Analysis (IPA) and Gene Set Enrichment Analysis (GSEA).

2. In Vivo Studies:

Exploratory Behavior and Spontaneous Locomotor Activity

Exploratory behavior and locomotor activity were assessed using the open field test as described previously (36). Briefly, the mouse was placed in an open field arena consisting of a white opaque plastic box 40 cm (L) X 40 cm (W) X 40 cm (H) divided into a central zone that measured 20 cm (L) X 20 cm (W) X 20 cm (H) and a periphery. Exploratory behavior was tracked during a 60 min unique trial using the Ethovision 10.5 animal tracking system (Noldus, Leesburg, VA). The total distance travelled (cm) in the center versus periphery as well as the average velocity (cm/s) were analyzed for treated and untreated groups. Data were collected as time bins of 10 minutes and as a total over the course of the experiment.

Motor Coordination

Motor coordination was investigated using the rotarod test (Med Associates, Fairfax, VT) using two different protocols (fixed speed on day 1 and accelerating speed on day 2). Prior to testing with the fixed speed protocol on day 1, each mouse was given 2 x 120 s practice sessions at 16 RPM. After practice, mice were tested at three different fixed speeds (16 RPM, 24 RPM then 32 RPM) for two 120 s trials at each speed and with an inter-trial interval of 15 min. On day 2, mice were tested in two trials under conditions of increasing difficulty in which the speed of the rotation gradually increased from 4 to 40 RPM over a 5-minute period. The time to fall was recorded in seconds and analyzed for each mouse.

Hippocampal-Dependent Memory

Hippocampal-dependant memory was analyzed using the fear conditioning test in a conditioning chamber with stainless-steel grid floor, equipped with an electric aversive stimulator, and house light, enclosed within a sound attenuating cubicle with exhaust fan (Med Associates, Fairfax, VT). On day one (training session), each mouse was individually placed for 5 min into the conditioning chamber and allowed to explore freely (habituate) for 180 seconds. Following exploration/habituation, two mild foot shocks (0.5 mA for 2 s) were administered at 180 s and 240 s. On day two (testing session), the mice were placed into the identical conditioning chamber for 5 min with no foot shocks. Each mouse was monitored for freezing (fear) behavior. The extent (or percent) of freezing was used as a measure of the animal's memory and analyzed as time bins of 60 s and as a total over the course of the experiment using the Freeze View software (Med Associates, Fairfax, VT).